Organic Geochemistry 200 (2025) 104922

Contents lists available at ScienceDirect

Organic Geochemistry

journal homepage: www.elsevier.com/locate/orggeochem

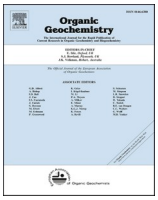

The giant barrel sponge *Xestospongia muta* takes up dissolved organic matter from benthic cyanobacterial mats

Lauren K. Olinger [a,b], Wendy K. Strangman [c], Steven E. McMurray [d], Ralph N. Mead [e], Joseph R. Pawlik [a,*]

[a] Department of Biology and Marine Biology, University of North Carolina Wilmington, Wilmington, NC, USA
[b] Center for Marine and Environmental Studies, University of the Virgin Islands, St. Thomas, VI, USA
[c] Department of Chemistry and Biochemistry, University of North Carolina Wilmington, Wilmington, NC, USA
[d] Old Woman Creek National Estuarine Research Reserve, Ohio Department of Natural Resources, Huron, OH, USA
[e] Department of Earth and Ocean Sciences, University of North Carolina Wilmington, Wilmington, NC, USA

ARTICLE INFO

Guest Editor — Hussain Abdulla

Keywords:
Porifera
Benthic-pelagic coupling
Dissolved organic matter
Metabolomics
Chemical defense
Organohalides

ABSTRACT

With the decline of reef-building corals, other organisms are taking over Caribbean reefs, including sponges and benthic cyanobacterial mats (BCM). Sponges take up dissolved organic matter (DOM), but the sources and chemical characteristics of DOM taken up by sponges are unknown. One likely DOM source is benthic autotrophs, including BCM, which are prolific producers of DOM. We tested the hypothesis that sponges take up BCM-derived DOM using laboratory experiments in which seawater samples were collected before and after sequential incubations of BCM and small individuals of the giant barrel sponge *Xestospongia muta*. The concentration of DOC and relative abundance of individual features in the high resolution mass spectra using untargeted metabolomics were determined for each sample. There was a significant increase in DOC after BCM incubations, followed by a significant decrease after sponge incubations. These changes were mirrored in single feature relative abundances, with 2101 out of 3667 features significantly enriched during BCM incubations, and 54% of these (1142) depleted during sponge incubations. Among BCM-enriched and sponge-depleted features, many were halogenated, some were known BCM-derived secondary metabolites (e.g., carriebowmide, barbamide), and others matched unidentified sponge-depleted features from seawater samples collected on the reef. To our knowledge, this is the first report that sponges take up BCM exudates, including some that were detectable in reef DOM, revealing a path of molecules from source to sink through their environment. The BCM exudates taken up by sponges may be used as a food source or incorporated into sponge secondary metabolites for holobiont maintenance or chemical defenses.

1. Introduction

Caribbean coral reefs are changing rapidly with non-reef building organisms replacing stony corals (Hughes 1994; Aronson et al. 2002; Maliao et al. 2008; Loh et al. 2015). One such group overtaking fore-reefs is sponges, a group characterized by complex aquiferous systems used to pump seawater while consuming particulate and dissolved carbon resources from it. The uptake of dissolved organic carbon (DOC) by sponges was experimentally proposed 50 years ago (Reiswig 1974), and research has since repeatedly confirmed the high contribution of DOC to the diets of many sponge species (Yahel et al. 2003), including *Xestospongia* spp. for which DOC represents the main source (60–96%) of dietary carbon (McMurray et al. 2016; Hoer et al. 2018; Wooster et al. 2019).

DOC represents the largest reduced carbon reservoir in the ocean at 600 Gt C. Free-living microbes process this DOC, transforming it from labile to recalcitrant forms, and in doing so create a global pump of carbon to the deep ocean (Jiao et al. 2014; Carlson and Hansell 2015). In the water column, the consumption of some of these microbes by protists results in cycling of DOC back into the food web in a major trophic pathway known as the "microbial loop" (Azam et al. 1983). A more recent "sponge loop" hypothesis proposes that sponges on coral reefs

* Corresponding author.
E-mail addresses: lauren.olinger@uvi.edu (L.K. Olinger), strangmanw@uncw.edu (W.K. Strangman), steven.mcmurray@dnr.ohio.gov (S.E. McMurray), meadr@uncw.edu (R.N. Mead), pawlikj@uncw.edu (J.R. Pawlik).

https://doi.org/10.1016/j.orggeochem.2024.104922
Received 30 April 2024; Received in revised form 9 December 2024; Accepted 18 December 2024
Available online 19 December 2024

play a similarly important role in cycling carbon back to the benthos by taking up DOC and converting it to detritus or biomass that is available to grazers (de Goeij et al. 2013; McMurray et al. 2018).

The sponge loop hypothesis was based on laboratory and field experiments with thinly-encrusting sponge species, including *Halisarca caerulea* (de Goeij et al. 2013). Although initially described as a "bacterial-containing" sponge (de Goeij et al. 2008b), more recent descriptions of *H. caerulea* have placed this species among the group with low microbial abundance (Moitinho-Silva et al. 2017; Campana et al. 2021). The first evidence of sponges consuming DOC came from carbon budget deficiencies in the particulate diets of sponge species with abundant microbial symbionts (i.e., bacteriosponges, sensu Reiswig 1981), prompting the conclusion that the remaining carbon was acquired from the DOC by those microbial symbionts. DOC is an uncommon dietary resource for metazoans, but is readily consumed by prokaryotic microbes, including those that comprise a substantial portion of the biomass of the sponge holobiont (Taylor et al. 2007).

Sponge species may be categorized as high or low microbial abundance (HMA, LMA), where HMA species have more diverse and abundant (by 2–4 orders of magnitude) microbial communities (Hentschel et al. 2003) and host specific taxa not found in seawater (Taylor et al. 2007). *Xestospongia muta* is an HMA species with a diverse microbiome, including photosynthetic Cyanobacteria (Fiore et al. 2013; Evans et al. 2021). The microbiome of HMA species may play roles in DOC uptake and nitrogen fixation (Weisz et al. 2007; Hoer et al. 2018; McMurray et al. 2018) as well as carbon fixation and biosynthesis of defensive metabolites and vitamins (Rubin-Blum et al. 2019; reviewed in Freeman et al. 2021).

The DOC taken up by the sponge holobiont is part of a larger mixture of dissolved organic matter (DOM) present in seawater. Advancements in high resolution liquid chromatography mass spectrometry (LC-MS)-based metabolomics and new tools for analyzing mass spectrometric data are refining annotation and classification of individual mass features representing individual metabolites and improving our understanding of the composition and dynamics of DOM (Kido Soule et al. 2015; Dührkop et al. 2021; Wegley Kelly et al. 2022). Early studies of coral reef DOM showed a potential core DOM profile across sites (Weber et al. 2020), but shifts in benthic communities (e.g., from coral- to macroalgae-dominant) can change the composition of DOM, which may lead to further microbialization of reefs (Haas et al., 2016; Wegley Kelly et al. 2022). Sponges also change the composition of DOM, as shown by previous metabolomics-based analyses of DOM from seawater going into and coming out of (incurrent and excurrent, In/Ex) sponges *in situ* (Fiore et al. 2017; Letourneau et al. 2020). These studies expanded on previous studies indicating that sponges prefer organic material from benthic sources (van Duyl et al. 2011) and prefer algal-derived over coral-derived DOM (Rix et al. 2017), although this may also depend on DOM availability (van Duyl et al. 2018).

Motivated by studies that combined In/Ex sampling and metabolomics analyses, we previously conducted extensive In/Ex field experiments on the fore-reef off Carrie Bow Cay in Belize, sampling 6 sponge species (3 each HMA and LMA) with 3–7 replicates per species over two years and investigated sponge alteration of DOM composition on a molecular level (Olinger et al. 2021). We observed that only the HMA sponge species took up DOM and altered the overall DOM profile, while their LMA counterparts had no observable effect on the DOM profile (Olinger et al. 2021). This HMA-LMA difference supports microbially-mediated processing of DOM by HMA species, which is in agreement with previous reports that HMA species are sinks of DOC (McMurray et al. 2018), and also in line with studies documenting that the HMA microbiome can process substantially more DOM than the LMA microbiome (Rix et al. 2020). Previous In/Ex experiments also showed that HMA sponges took up a disproportionate number of halogenated metabolites, raising questions about the origins and possible uses of these metabolites by the sponge. The HMA holobiont may take up bioactive metabolites produced by other organisms to potentially use as secondary metabolites (e.g., chemical defenses) or as a food source (Olinger et al. 2021). One source of this DOM may be benthic cyanobacterial mats (BCM) that are proliferating on some Caribbean coral reefs (de Bakker et al. 2017; Ford et al. 2018). BCM comprise a group of filamentous species, including *Moorea producens* (formerly *Lyngbya majuscula*) which is a prodigious source of secondary metabolites in the Caribbean and elsewhere, including many that are halogenated (Arif et al. 2012).

Given the increasing abundance of both BCM and sponges on Caribbean fore-reefs, and the potential consequences of their interactions, it is important to determine whether DOM may be exchanged between BCM and sponges and to identify the types of metabolites involved in this transfer. In this study, we used laboratory experiments followed by molecular characterization of DOM to investigate whether sponges take up BCM exudates, and if so, to determine the molecular traits of DOM that may be involved.

2. Methods

2.1. Experiment preparation

Laboratory incubation experiments of benthic cyanobacterial mats (BCM) and sponges in seawater (n = 5) were conducted at the Smithsonian Carrie Bow Cay field station, 12–16 March 2020. The BCM (primarily *Moorea producens*, formerly *Lyngbya majuscula)* and sponge pieces (approximately fist-sized individuals of *Xestospongia muta*) were gathered on the fore-reef (10–20 m depth) and allowed to heal for at least 12 h. Cone-shaped sponge pieces were cleanly sliced with a sharp knife from the top of slightly larger individuals so that no substratum was included in replicate individuals. Each day, the specimens and seawater were collected, including one *X. muta* individual (118.9 – 178.6 g wet weight), tufts of BCM (26.1 – 34.6 g wet weight), and 8 L of seawater, and immediately (approx. 10 min) transported to the lab at Carrie Bow Cay. Seawater was filtered (0.7 μm GFF) and a portion (approx. 2 L) was used to periodically flush the BCM and sponges before incubations. To maximize replication of treatments in limited time at a field site, we dispensed with sponge-free controls (see Discussion). For a detailed description of experimental preparation, see the Supporting Information.

2.2. Experimental procedure

The BCM was transferred to a glass incubation vessel containing the remaining 6 L filtered seawater and a bubbler, and a 1200 ml "pre-BCM" seawater sample was immediately collected via siphon by PTFE tubing (Fig. 1a). The vessel was covered with a glass plate and LED aquarium light (Kessel A360WE Tuna Blue), exposing the BCM to 1000 μmol photons m^{-2} s^{-1} of light (Fig. 1b). After 2 h, a 1200 ml "post-BCM" seawater sample was collected (Fig. 1c). Then, 3 L of seawater was siphoned via PTFE tubing from the BCM incubation vessel to the sponge incubation vessel, within which the sponge in its original collection vessel had been placed following several flushes with filtered seawater to the point of overflow to avoid exposing the sponge to air and to rinse off external surfaces of the vessel. A 1200 ml "pre-sponge" seawater sample was collected (Fig. 1d), and the vessel was covered with foil and placed in the dark (Fig. 1e). After 2 h, a "post-sponge" sample was collected (Fig. 1f), and sponge pumping was confirmed after experimental runs using fluorescein dye. Experimental controls (n = 5) were prepared following each experiment by passing 600 ml ultrapure water (Honeywell) through the filtration apparatus and incubation vessels and analyzed alongside experimental samples for post-processing removal of contaminants.

Samples from experimental timepoints (pre-BCM, post-BCM, pre-sponge, post-sponge) and controls were filtered immediately after collection (0.2 μm PTFE filter, Omnipore). 20 ml of the filtrate was transferred into a scintillation vial (Traceclean, VWR) with 100 μl 50%

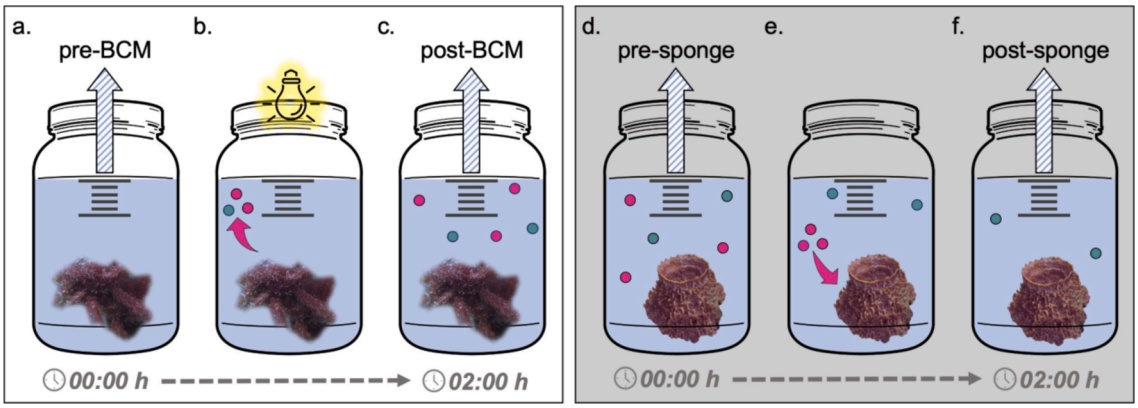

Fig. 1. Schematic of the lab experiment procedure. The experiment began with a) the addition of BCM to a vessel of filtered seawater and collection of 1200 ml pre-BCM seawater sample, followed by b) the 2 h incubation resulting in DOM production (pink and green dots) and then c) the collection of 1200 ml post-BCM seawater sample. The seawater containing BCM-exudate was then transferred to a second vessel with a sponge, and d) the 1200 ml pre-sponge seawater sample was collected, followed by e) the 2 h incubation of the sponge, including hypothesized uptake of BCM exudates (pink dots), and finally f) the collection of the 1200 ml post-sponge seawater sample.

phosphoric acid and stored in the refrigerator (4 °C) for later quantification of bulk DOC. The remaining 1 L of the 0.2 μm filtrate was acidified to pH 2 using hydrochloric acid (Honeywell) in preparation for solid phase extraction. See the Supporting Information for a more detailed experimental procedure.

2.3. Bulk DOC

The 20 ml samples were transported in coolers on ice to University of North Carolina Wilmington (UNCW) for quantification of bulk DOC using high-temperature catalytic oxidation with a Shimadzu TOC 5050 analyzer (McMurray et al. 2016, 2018). The normality of bulk DOC data was confirmed using the Shapiro-Wilk test ($p = 0.16$) and visualized using a Q-Q plot, thus subsequent analyses proceeded with raw DOC values. DOC concentrations were compared across experimental timepoints (pre-BCM, post-BCM, pre-sponge, post-sponge) using repeated measures analysis of variance (ANOVA), followed by post-hoc paired t-tests with Benjamini–Hochberg corrected p-values to evaluate pairwise differences between the timepoints.

2.4. Solid phase extraction

Solid phase extraction (SPE) was used to extract DOM from the acidified 1 L samples on the same day that samples were collected. The SPE procedures followed established methods (Dittmar et al. 2008; Olinger et al. 2021) and are described in more detail in the Supporting Information. Briefly, each 1 L sample was passed through a preconditioned SPE cartridge (1 g/ 6 cc PPL, Agilent BondElut), followed by DOM elution with 6 mL methanol into scintillation vials (Traceclean, VWR). Vials were stored at −20° C until transported on ice in coolers to UNCW for analysis using liquid chromatography high resolution mass spectrometry (LC-MS).

2.5. Data acquisition and preprocessing

Data acquisition and preprocessing were conducted as described previously (Olinger et al. 2021) and in more detail in the Supporting Information. Briefly, samples were analyzed using an ACQUITY I-Class UPLC (Waters, USA) coupled to a Xevo G2-XS QToF mass spectrometer (Waters, UK) with an electrospray ionization (ESI) source operated in positive mode. Raw data were converted using MSConvert (Chambers et al. 2012) for peak picking and feature list generation in R using *xcms* (Smith et al. 2006) and *CAMERA* (Kuhl et al. 2012; SI Figure 2a). Each feature represented an MS^1 peak with a unique *m/z* and retention time corresponding to an individual compound in the seawater and with relative abundances approximated by the integrated peak area. Feature lists were filtered as described in the Supplementary Information to remove contaminants and uncommon features, leaving 3667 features on which the following statistical analyses were conducted.

2.6. Analyses of MS^1 features

Feature abundances were normalized to bulk DOC concentrations and range-scaled, and principal component analysis (PCA) was used to evaluate unsupervised groupings among the experimental timepoints (pre-BCM, post-BCM, pre-sponge, post-sponge; SI Figure 2b). Repeated measures ANOVA was used to compare normalized, log-transformed feature abundances across the experimental timepoints, with Benjamini-Hochberg corrections for false discovery rates. For the features with significant differences ($p < 0.05$), pairwise comparisons were performed using paired t-tests and Benjamini–Hochberg corrected p-values to evaluate within-group differences among the experimental timepoints. Features were assigned significance categories for BCM and sponge incubations, with “enriched” features having increased and “depleted” features having decreased from pre- to post- timepoints (SI Figure 2c), and significance categories were appended to the feature lists for subsequent analyses (SI Figure 2d).

2.7. Component features

Raw data were imported into UNIFI (Waters, US) for componentization to generate fragmentation spectra and screen against the 3667 MS^1 features (SI Figure 2e-f; Olinger et al. 2021). The 2925 components that matched to features are henceforth referred to as component features (SI Figure 2g). The componentization process also tested spectra against theoretical isotope distributions to indicate presence of halogens (Br, Br_2, Br_3, Cl, Cl_2, Cl_3) with at least 90% confidence (SI Figure 2h).

2.8. BCM secondary metabolites

Component features were screened against a custom library of 298 secondary metabolites that were listed in NPAtlas (van Santen et al. 2022) as being derived from *Moorea producens* or *Lyngbya majuscula*, as the species was previously named. The structures included in this library facilitated matching of theoretical substructures and fragments in componentized MS^E spectra (SI Figure 2i). Extractions were also performed on the BCM tissue collected after each experimental run, and more detailed extraction methods can be found in the Supporting

Information. Extracts were analyzed with LC-MS and screened in UNIFI against component features and the libraries of BCM secondary metabolites. Potential matches were verified with MS/MS analysis of tissue extracts to produce unequivocal fragmentation patterns (Level 3 identifications; Schymanski et al. 2014).

2.9. Chemical classifications

The high energy fragment peaks of 2925 component features were analyzed in SIRIUS 4 (Dührkop et al. 2019) for classification using the submodule CANOPUS (Class Assignment aNd Ontology Prediction Using mass Spectrometry; SI Figure 2j; Dührkop et al. 2021). See the Supporting Information for more details about the analysis and parameters used in this classification. The 1872 features with assigned classifications based on the ClassyFire chemontology (Djoumbou Feunang et al. 2016) were used to compare DOM that was enriched or depleted during BCM and sponge incubations. The chemodiversity of enriched and depleted DOM was compared using Shannon diversity indices, which consider both diversity and evenness and have been used previously to estimate chemodiversity (Pielou 1966; Noriega-Ortega et al. 2019).

2.10. Recurrent features

The 2925 component features were screened against another metabolomics dataset that had been generated with the same LC-MS methods, instruments, and sample apparatuses as the present study (SI Figure 2k). This dataset comprised DOM in In/Ex samples collected from sponges on the Carrie Bow Cay fore-reef in 2018 (n = 3 each from 6 sponge species) and 2019 (n = 7 each from 2 sponge species; Olinger et al. 2021). Comparison of these two datasets (the laboratory experiments herein and In/Ex sampling in Olinger et al. 2021) was used to detect features that were depleted by sponges in both environments, as these would indicate metabolites of known origin (e.g., BCM if significantly enriched during BCM incubations) and ecological relevance due to their detectable quantities in coral reef DOM. Any features that were depleted in the In/Ex samples of at least one sponge species per year are hereafter referred to as recurrent features. For each suspected recurrent feature, In/Ex feature abundances of all 2018 and 2019 In/Ex samples were log2 transformed and compared using paired t-tests with Benjamini–Hochberg corrected p-values. All statistical tests were performed in R (R Core Team 2020).

3. Results

3.1. Bulk DOC

Concentrations of DOC differed significantly over the duration of the experiments ($F_{3,\ 12} = 16.155$, $p < 0.001$, $\eta^2_G = 0.7$). Pairwise tests revealed a significant increase in DOC during BCM incubations, with average (± SE) concentrations rising from 95.7 ± 2.8 μmol C/L (pre-BCM) to 142.2 ± 5.8 μmol C/L (post-BCM). Concentrations of DOC also decreased significantly during sponge incubations, with mean values dropping from 130 ± 7.3 μmol C/L (pre-sponge) to 97.4 ± 8.6 μmol C/L (post-sponge). Concentrations of DOC fluctuated in equal but opposite directions during BCM and sponge incubations, and final concentrations (post-sponge) were statistically indistinguishable from initial values (pre-BCM; Fig. 2a).

3.2. Analyses of MS^1 features

The PCA biplots used to explore groupings based on the relative abundances of 3666 mass features are shown with arrows connecting timepoints of individual BCM and sponge incubations (Fig. 3). The blue arrows that signify the BCM incubations all point upwards, while the orange arrows that signify the sponge incubations all point downwards, mirroring the bulk DOC analyses and further suggesting a uniform

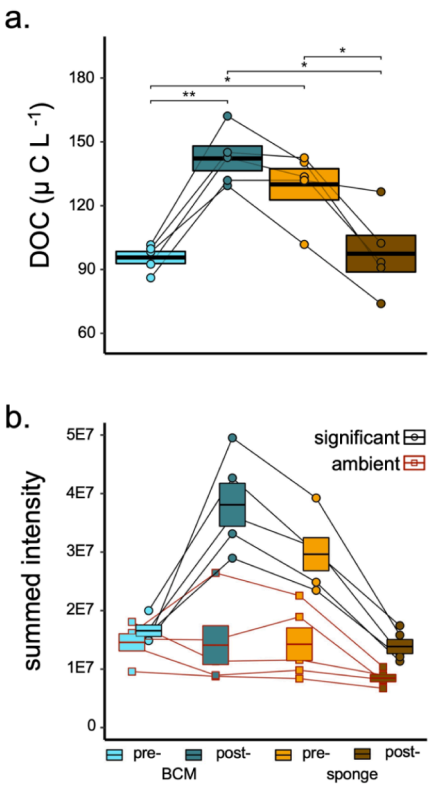

Fig. 2. Changes to DOC and DOM during the experiment. Boxes show mean ± SE, and lines connect individual values from each of the 5 experimental runs. a) Bulk DOC, with asterisks indicating significant differences from pairwise tests. b) Summed MS^1 intensities of ambient features outlined in red and significant (BCM-enriched and/or sponge-depleted) features outlined in black. Slight decreases between post-BCM and pre-sponge samples are likely due to depletion by sponge during the collection of the pre-sponge sample, and this decrease was not statistically significant, as seen in panel a.

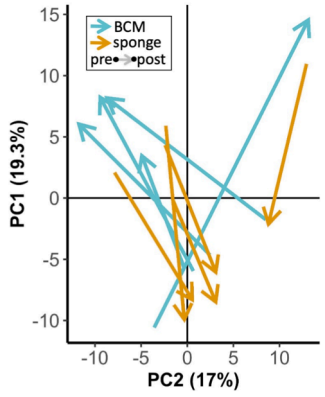

Fig. 3. PCA showing changes to the DOM profile across experimental timepoints. Arrows connect pre- and post- timepoints of individual BCM (blue) and sponge (orange) incubations.

change to the DOM during BCM incubations, followed by a reversal during sponge incubations.

Repeated measures ANOVAs were used to compare relative abundances of single features across timepoints for categorization as enriched, depleted, or ambient (i.e., unchanged, following existing terminology; Wegley Kelly et al. 2022). During BCM incubations, 2102 features were enriched, zero features were depleted, and 1565 features were unchanged. During sponge incubations, one feature was enriched,

1347 features were depleted, and 2319 features were unchanged. There was considerable overlap (54%) between features that were enriched during BCM incubations and depleted during sponge incubations, with a total of 1142 features hereafter categorized as "BCM-enriched/sponge-depleted". The remaining 1360 features that were not significantly changed during BCM or sponge incubations were categorized as "ambient" (Table 1).

MS1 chromatogram intensities were normalized to bulk DOC values in each sample. Such sample-based normalization of metabolomics data can reduce variance (Sun and Xia, 2023), including that caused by fluctuations in DOC that occurred during the experiment. This approach was more relevant than normalizing all samples to the same arbitrary constant, which could distort individual feature abundances based on abundances of other features. For this normalization approach to be valid, biological processes—specifically, metabolite production by BCM and depletion by actively pumping sponges in the closed experimental system—needed to have greater influence on peak intensities than analytical artifacts from sample processing; this ensures meaningful correspondence between MS1 peak intensities and the bulk DOC values to which they are normalized. Several validation steps were taken to ensure observed feature changes were more attributable to underlying metabolite changes than artifacts of extraction or transformation methods.

First, we duplicated the repeated measures ANOVA on non-normalized, log-transformed feature abundances. Analysis of the non-normalized data revealed patterns consistent with our DOC-normalized results (SI Table 1). Among significantly changed features, sponge depletion was most common (683 features; 18.6%), with 305 of these features (8.3%) also showing BCM enrichment. In contrast, few features showed patterns counter to trends in DOC-normalized data: only 19 features (0.5%) were depleted during BCM incubations and 30 features (0.8%) were enriched during sponge incubations. These counter-trending features may represent true biological signals or a minimal proportion (<1%) of false positives in non-normalized data. The consistency between normalized and non-normalized data was further supported by similar DOM signatures in PCA biplots (Fig. 3; SI Figure 3).

General trends in individual feature abundances were consistent between normalized and non-normalized data (e.g., SI Figure 4), despite greater variance in non-normalized data contributing to the classification of most features as ambient, or without significant changes during the experiment (2844; 78%; SI Table 1). Furthermore, several sponge-depleted features found in Olinger et al. (2021), which did not normalize to DOC, were also identical to sponge-depleted features herein (i.e., recurrent features). Negligible sponge-enriched features were also reported in Olinger et al. (2021), consistent with the results herein.

Finally, the raw (non-transformed) peak intensity of significant features tracked total DOC concentrations (Fig. 2B); this figure, modeled after Wegley Kelly et al. (2022), demonstrates that the DOM changes detected by mass spectrometry analysis proportionally reflect the overall shifts in DOC concentration across treatments, suggesting a consistent representation of the significant features in the analytical approach. While spurious categorizations of features due to ionization or extraction biases cannot be entirely ruled out, and we cannot dismiss the chance of having missed classes of important features, such as organic acids and sugars produced abundantly by BCM but negligibly retained on SPE columns (Nelson et al. 2016; Wegley Kelly et al. 2022), the analysis was careful to address potential artifacts associated with sample extractions and transformation methods.

Table 1
The number of features in each significance category (depleted, enriched, or ambient) during BCM and sponge incubations. Numbers in parentheses represent number of features in the subset of 2925 features that were matched to components in UNIFI (i.e., component features). BCM-amb and sponge-amb indicate features that were not significantly changed during BCM incubations or sponge incubations, respectively. The single sponge-enriched feature is omitted from this table.

	sponge-depleted	sponge-amb	total
BCM-enriched	1142 (1030)	959 (737)	2101 (1767)
BCM-amb	205 (154)	1360 (1003)	1565 (1157)
total	1347 (1184)	2319 (1740)	3666 (2924)

3.3. Component features

The 2924 component features included 1030 BCM-enriched/sponge-depleted features, 154 sponge-depleted features, 737 BCM-enriched features, and 1003 ambient features (Table 1). A total of 164 component features (5.6%) contained halogens, including 62 (6%) of BCM-enriched/sponge-depleted component features. Monochlorines (Cl) were disproportionately abundant among sponge-depleted component features, relative to all component features, including 45 (4.3%) of the BCM-enriched/sponge-depleted component features. A number of sponge-depleted component features also matched to Cl_2 (n = 9) and Cl_3 (n = 11), and several of these were also BCM enriched (n = 5 Cl_2, n = 6 Cl_3; SI Table 2).

3.4. BCM secondary metabolites

Screening against the custom structure library of 298 secondary metabolites derived from *M. producens* revealed putative matches to five component features (Table 2). Two (carriebowmide and pre-carriebowmide) matched to BCM-enriched/sponge-depleted component features (Fig. 4 a and b), and three (barbamide, hectochlorin, deacetylhectochlorin) matched to sponge-depleted component features (Fig. 4 c–e). The three features classified as sponge-depleted (Fig. 5 c–e) show increases in abundance during BCM incubations, though these increases were inconsistent across experimental runs. The three compounds matching sponge-depleted component features (barbamide, hectochlorin, deacetylhectochlorin) were also halogenated. The halogen assignments in UNIFI, based on isotope patterns, matched the molecular formulae of the compounds, providing independent support for these identifications.

The five putatively matched compounds were also present in BCM tissue extracts. The MS/MS of tissue extracts revealed fragmentation patterns similar to those in the DOM, and the alignment of MS^E spectra from the DOM sample and MS/MS spectra from the BCM tissue extract for each compound are shown in SI Figure 5-9. Several MS/MS fragments also matched to theoretical substructures of each suspected compound (panel d of SI Figure 5-9).

3.5. Chemical classifications

The 1872 component features with chemical classifications included 599 BCM-enriched/sponge-depleted features, 90 sponge-depleted features, 562 BCM-enriched features, and 621 ambient features. Pie charts revealed a similar composition of CANOPUS superclasses among the four groups of DOM, with all dominated by organic acids and derivatives (46–51%), followed by lipids and lipid-like molecules (17–24%; SI Figure 10). Associated subclass assignments revealed some differences among the groups of DOM (SI Table 3). The dominant subclass, "amino acids, peptides, and analogs" represented > 40% of DOM depleted during sponge incubations (42.1% in BCM-enriched/sponge-depleted, 41.1% in sponge-depleted), which was slightly greater than that of BCM-enriched (38.6%) and ambient DOM (35.6%). Some other noteworthy patterns emerged among rarer subclasses. For example, those classified as depsipeptides were 4x more abundant in BCM-enriched/sponge-depleted DOM than BCM-enriched DOM (1.8% vs 0.4%), and depsipeptides were absent altogether from sponge-depleted DOM (SI Table 3). Shannon diversity indices revealed a lower chemodiversity in

Table 2
BCM secondary metabolites that were depleted during sponge incubations. Column halo refers to halogenation indicated in UNIFI, and halogenation assignments were independent of molecular formulae (column MF).

significance	compound	MF	halo	structure
BCM-enriched/ sponge-depleted	carriebowmide	$C_{46}H_{68}N_6O_9S$	–	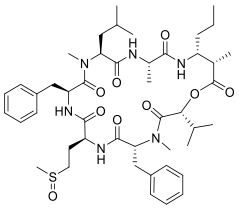
BCM-enriched/ sponge-depleted	precarriebowmide	$C_{46}H_{68}N_6O_8S$	–	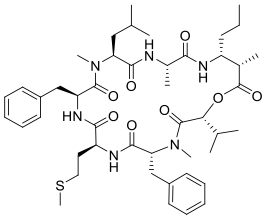
sponge-depleted	barbamide	$C_{20}H_{23}Cl_3N_2O_2S$	Cl_3	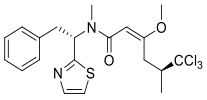
sponge-depleted	hectochlorin	$C_{27}H_{34}Cl_2N_2O_9S_2$	Cl_2	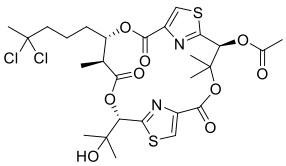
sponge-depleted	deacetylhectochlorin	$C_{25}H_{32}Cl_2N_2O_8S_2$	Cl_2	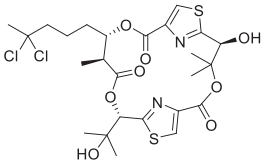

DOM that was depleted during sponge incubations (H = 1.70 for sponge-depleted DOM; H = 1.78 for BCM-enriched/sponge-depleted DOM) compared to BCM-enriched DOM (H = 1.92) and ambient DOM (H = 2.09; SI Table 3).

3.6. Recurrent features

Comparison of two DOM datasets in UNIFI revealed 10 recurrent features that were depleted by *X. muta* during the lab experiments herein and by at least one HMA sponge species during previous In/Ex sample collections (Olinger et al. 2021; Table 2). See Fig. 5 for boxplots showing In/Ex abundances of two recurrent features, and boxplots for all 10 recurrent features are shown in SI Figure 11. Among the seven BCM-enriched/sponge-depleted features, five were significantly depleted by multiple HMA species, including two that were chlorinated based on theoretical isotope distributions. Interestingly, two BCM-enriched/sponge-depleted features were depleted only in the In/Ex samples of *X. muta* and were unchanged in the In/Ex samples of other sponge species. The three additional recurrent features were categorized as sponge-depleted in the present study and included two depleted by multiple HMA species and one depleted only by *X. muta* in In/Ex samples. Notably, none of the recurrent features were depleted in In/Ex samples of low microbial abundance (LMA) sponge species.

4. Discussion

While significant progress has been made in characterizing coral reef DOM in recent years through the efforts of numerous researchers (e.g., Haas et al., 2010; Nelson et al., 2013; Kido Soule et al., 2015; Fiore et al., 2017; van Duyl et al., 2018; Weber et al., 2020; Wegley Kelly et al., 2022), the sheer complexity and biodiversity of these ecosystems, coupled with the rapid turnover of DOM, means that our understanding of DOM sources and dynamics on coral reefs remains incomplete. The present study contributes to this growing body of knowledge by examining the transfer of DOM from benthic cyanobacterial mats (BCM) to sponges, two increasingly abundant groups on Caribbean coral reefs. Sponges change the molecular composition of DOM as they pump seawater (Fiore et al. 2017; Letourneau et al. 2020; Olinger et al. 2021). The present study found that a portion of DOM is transferred from benthic cyanobacterial mats (BCM) to sponges, two increasingly abundant groups on Caribbean coral reefs. Further, this study connects unidentified DOM compounds across two datasets, one from samples collected in the field in 2018 and 2019, the other from samples collected in a laboratory setting in 2020, demonstrating the value of such recurrent features to better understanding DOM sources and sinks.

The DOM produced by BCM likely consists of overflow photosynthetic byproducts, metabolites originating from cyanobacterial cell lysis, and secondary metabolites (Brocke et al. 2015), the uptake of which may be mediated by microbial symbionts within the sponge. This experiment was conducted using one sponge species, the high microbial abundance (HMA) species *Xestospongia muta*. This species was chosen because of its abundance on the Carrie Bow Cay fore-reef (Villamizar et al. 2014) and elsewhere (e.g., Florida Keys, McMurray et al. 2015) and because of previous findings that only HMA species took up DOM

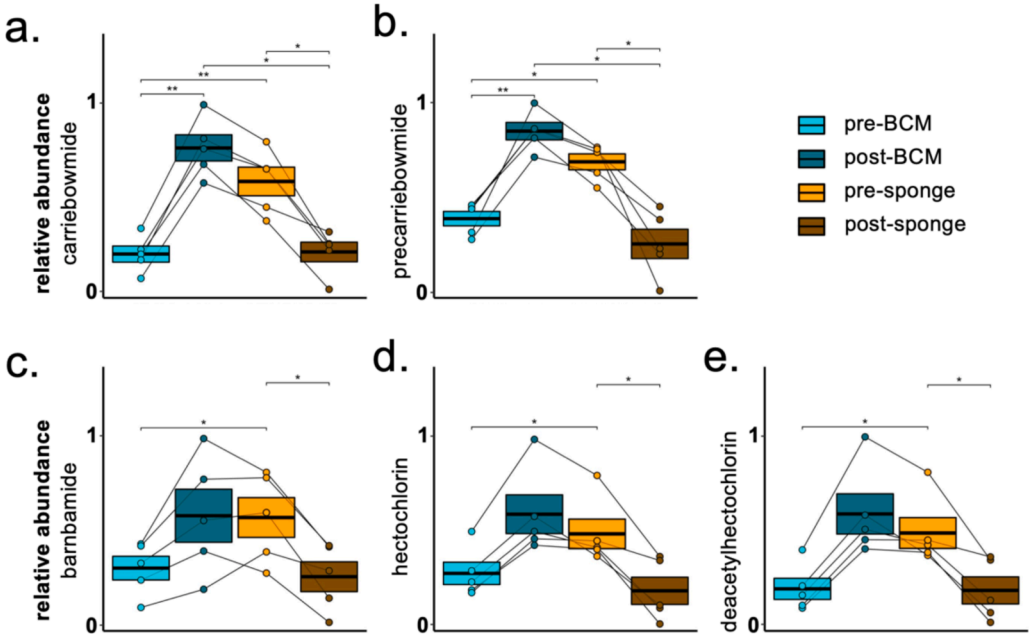

Fig. 4. Relative abundances of significant features with matches to BCM secondary metabolites. Metabolite matches included BCM-enriched/sponge-depleted features matching to a) carriebowmide and b) precarriebowmide, and sponge-depleted features matching to halogenated c) barbamide, d) hectochlorin, and e) deacetylhectochlorin. Boxes show mean ± SE, and lines connect individual values from each experimental run. Asterisks indicate significant differences from pairwise tests. Slight decreases between steps 2 and 3 (post-BCM and pre-sponge, respectively) are likely due to depletion by sponge during the collection of the pre-sponge sample, but this decrease was not statistically significant for any of the features.

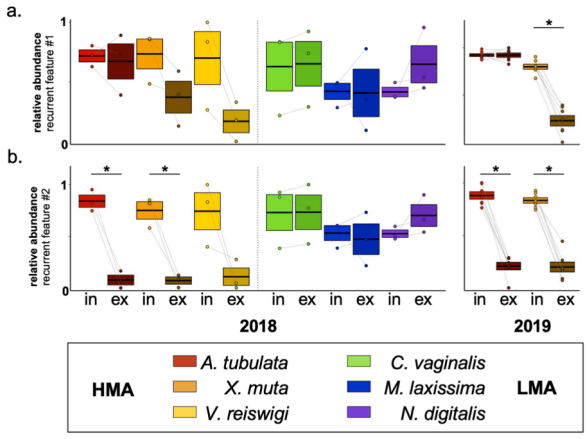

Fig. 5. Relative abundances of two of the 10 recurrent features in In/Ex samples (Olinger et al. 2021). Box-plots show the mean ± SE relative abundances from incurrent and excurrent samples of each species, with lines connecting the incurrent and excurrent samples from the same individual. Asterisks represent significant differences from paired t-tests. The features shown include a) the chlorinated BCM-enriched/sponge-depleted Feature #7 that was depleted only by *X. muta* and b) the BCM-enriched/sponge-depleted Feature #3 that was depleted by multiple HMA species. Feature IDs correspond to SI Table 4, and for box-plots of all 10 recurrent features, see SI Figure 11.

(Olinger et al. 2021). Microbially-mediated DOC uptake is at odds with some reports of DOC uptake by host sponge cells (Achlatis et al. 2019; Rix et al. 2020; Hudspith et al. 2021), but consistent with other findings showing that only HMA species are sinks of DOC (Hoer et al. 2018; McMurray et al. 2018). Inconsistencies may be due to differences in experimental methods and varying operational definitions of DOC with stricter methods generally resulting in an HMA-LMA divide indicative of microbially-mediated uptake of the molecular fraction of DOM (Olinger et al. 2021). Once assimilated, the HMA sponge holobiont may use or repurpose these compounds either as a food source or to for incorporation into secondary metabolites, including chemical defenses.

The BCM exudate may have been used as food by the sponge holobiont. Although the present study did not determine whether uptake was due to direct metabolism, sponges can take up labile compounds such as glycerol-3 phosphate and pantothenic acid (Fiore et al. 2017), and the sponge microbiome has genes related to metabolism of substances common in algae- and coral-derived DOM, such as starch, arabinose, fucose, and xylan (Robbins et al. 2021). DOC is an important component of the sponge diet (Pawlik and McMurray 2020), and much of this DOC likely originates from the substantial production by benthic autotrophs on coral reefs (Haas et al. 2010; Nelson et al. 2013; Brocke et al. 2015; Wegley Kelly et al. 2022). Barrel sponges may not consume DOC below a threshold concentration of 80 μmol C/L (Wooster et al. 2019), and this value was comparable to the average DOC concentration after sponge incubations herein (97.4 ± 8.6 μmol C/L) although whether this is a function of DOM quality (labile or recalcitrant) or quantity remains unclear.

On coral reefs, BCM exudate may also be used as a source of secondary metabolites by the sponge holobiont, with potential purposes as chemical defenses or signaling molecules. This was previously proposed following In/Ex experiments demonstrating that HMA sponges took up many halogenated features from seawater DOM (Olinger et al. 2021) and the well validated prevalence of halogenation in chemical defenses (Laus 2001). The contribution of defensive secondary metabolites to DOM is unknown (Carlson and Hansell 2015) but may be significant in coral reefs where allelopathic interactions are common (Pawlik et al. 2007; Chadwick and Morrow 2011). Furthermore, the detected BCM secondary metabolites that were depleted during sponge incubations are known to have various bioactivities, including fish-deterrent properties of carriebowmide and precarriebowmide (Gunasekera et al. 2008; Mevers et al. 2013), molluscicidal properties of barbamide (Orjala and Gerwick, 1996), and antifungal properties of hectochlorin and deacetylhectochlorin (Marquez et al. 2002; Suntornchashwej et al. 2005).

Sponges may be opportunistically taking up defensive metabolites exuded by BCM for use in their own tissues. Kleptochemistry, or the co-

opting of chemical defenses, is used by some opisthobranch molluscs that feed on sponges and store bioactive sponge defensive metabolites in their own tissues, either unchanged or with modifications to prevent autotoxicity (Pawlik et al. 1988; Marín and Ros 2004; Winters et al. 2018). The stinging black sponge *Haliclona cnidata* engages in kleptocnidism, or the stealing of precursor nematocyst stinging cells from nearby cnidarians (Schellenberg et al. 2019).

At least 40 metabolites have been identified from *X. muta* tissue extracts (Schmitz and Gopichand 1978; Shimura et al. 1994; Morinaka et al. 2007; Zhou et al. 2011), but the chemical defenses of *X. muta* vary over depth and with seasons, perhaps due to fluctuating availability of defensive metabolite precursors in the environment (Chanas and Pawlik 1997; Villegas-Plazas et al. 2019; Bayona et al. 2021). Sponges can modulate their pumping rates to optimize foraging efficiency, and they selectively feed on particulate organic matter and DOM from different sources (McMurray et al. 2016; Rix et al. 2017; Wooster et al. 2019; Hudspith et al. 2021). Chemical classifications in the present study showed that sponge-depleted DOM was less diverse than overall DOM and included classes such as depsipeptides that were absent in ambient DOM and exclusive to BCM-enriched features, providing further evidence of selectivity and perhaps opportunistic uptake of an uncommon resource.

The most novel finding from this study is the 10 recurrent features that were depleted by sponges in both the laboratory incubations reported herein and in the previous year's In/Ex field experiments from the Carrie Bow Cay fore-reef reported in Olinger et al. (2021). These recurrent features, including 7 BCM exudate metabolites, 3 of which were halogenated, represent ecologically relevant compounds and potentially valuable DOM resources for sponges. This study traces individual molecules from source (BCM) to sink (sponge) amidst the complexity of natural coral reef DOM. As molecular level characterization of coral reef DOM becomes more common (Weber et al. 2020; Wegley Kelly et al. 2022) this will produce a growing database of features cataloged in public repositories (e.g., MetaboLights, GNPS; Wang et al. 2016; Haug et al. 2017) that can be used for pattern mining to define a core profile of coral reef DOM. As emphasized in a previous review (Moran et al. 2016), the value of cataloging a minute fraction of persistent DOM components may be comparable to the value of genomic sequencing of a small subset of marine bacteria (175 taxa out of hundreds of thousands) which led to revolutionary insights into elemental cycling in the ocean (Yooseph et al. 2010).

The cross referencing of recurrent features with the In/Ex sample dataset also revealed that uptake of DOM features was due to specific microbiomes, not only across HMA and LMA species, but within HMA species, with some features depleted only by *X. muta* and others depleted also by *Agelas tubulata* and *Verongula reiswigi*. This specificity may be due to highly variable microbiomes across sponge species (Thomas et al. 2016). Importantly, at least two cryptic subspecies of *X. muta* with distinct microbiomes have been found in the Caribbean (Swierts et al. 2017; Deignan et al. 2018; Evans et al. 2021), thus any species-specific uptake by *X. muta* may be due either to microbiome similarities between the subspecies or sampling from only one of the subspecies.

Non-reef building organisms including BCM and sponges are becoming increasingly dominant on fore-reefs (Loh et al. 2015; de Bakker et al. 2017; Ford et al. 2018) with likely consequences for carbon cycles. A previous study found that the spread of BCM over sediment prevented the sediment from acting as a DOC sink, causing the reef to shift to a net source of DOC when BCM cover exceeded 19% (Brocke et al. 2015). Many sponges are significant DOC sinks (de Goeij et al. 2008a; McMurray et al. 2018), and sponge uptake of BCM-derived DOM may partly offset the shift caused by BCM-coverage of sediment, although the magnitude and types of DOC recycled by sponges versus sediment remain unknown. Additionally, a "vicious circle" has been hypothesized between sponges and BCM or other benthic photoautotrophs, whereby the autotroph provides DOC photosynthate to sponges, and sponges in turn provide nitrogenous wastes or other limiting nutrients to the autotroph (Pawlik et al. 2016).

The DOM transfer from BCM to sponges is one link in an extensive network of metabolite exchanges between benthic organisms. Metabolomics-based characterization of DOM can help resolve not only the characteristics and identities of metabolites, but also their sources and sinks. Each metabolite is represented by a mass feature, and each feature corresponds to a mass spectrum that, like a barcode, is unique and traceable even if nothing else is known about the metabolite that it represents. Statistical grouping of mass spectral features (e.g., BCM-enriched, sponge-depleted) produces fingerprints of DOM sources (e.g., BCM) that can be traced to DOM sinks (e.g., sponges) and across datasets (e.g., between laboratory and In/Ex experiments). A similar approach was recently used to make a library of unidentified ions in urine samples for connecting chemical components across datasets (Simón-Manso et al. 2019), and such a library could prove valuable for connecting unidentified, recurrent features across the vastness of marine ecosystems.

To maximize replication of treatments in limited time at a remote field site, this study lacked a sponge-free control in which seawater enriched in algal DOM was incubated without a sponge. Such a control would have assessed DOM depletion unrelated to sponge presence, particularly by seawater microbes remaining after filtration. However, we are confident that seawater microbes had a negligible effect on DOM for five reasons: (1) Incubations used 0.7 μm filtered seawater, greatly reducing free-living microbe abundance. (2) The remaining microbes in the filtrate are unlikely to significantly affect DOM over such short periods; similar studies with microbes occurred over multiple days (Pedler et al. 2014). (3) The absence of significantly depleted features during BCM incubations indicates minimal processing by free-living microbes, which were present in the same seawater subsequently used for sponge incubations. (4) Sponge pumping was confirmed after incubations, ensuring seawater processing during the 2 h period. (5) Recurrent features depleted by sponges in both these laboratory incubations and previous field In/Ex experiments (Olinger et al. 2021) implicate the sponge holobiont in feature depletion; free-living microbe effects were minimal in In/Ex samples, collected simultaneously and separated only by the sponge body wall.

While the LC-MS approach used in this study provides valuable insights, the detected DOM was constrained by extraction efficiencies (40–50%), and biases introduced by the PPL sorbent and positive ionization mode (Petras et al., 2017). Such limitations may result in underrepresentation of certain compound classes, for example the organic acids and sugars produced in abundance by BCM (Nelson et al. 2013; Wegley Kelly et al. 2022). Future studies employing alternative extraction methods and using both positive and negative ionization modes could provide an even more comprehensive characterization of DOM, potentially revealing additional metabolites involved in exchanges between sponges, BCM, and other benthic organisms.

5. Conclusion

We report herein that the HMA sponge *X. muta* took up BCM-derived DOM in the lab and under natural conditions on a coral reef. More work is needed to determine whether sponges take up BCM photosynthate and secondary metabolites (e.g., carriebowmide, barbamide, hectochlorin) for food or for repurposing into their own secondary metabolites, and the extent to which BCM-derived DOM is taken up by other sponge species. If food resources, defenses, or nutrients are readily exchanged among sponges and BCM or other benthic autotrophs, this could alter carbon cycles and drive further loss of reef-building corals.

CRediT authorship contribution statement

Lauren K. Olinger: Writing – original draft, Visualization, Methodology, Investigation, Formal analysis, Data curation, Conceptualization. **Wendy K. Strangman:** Writing – review & editing, Supervision,

Project administration, Methodology, Funding acquisition, Conceptualization. **Steven E. McMurray:** Writing – review & editing, Methodology, Investigation. **Ralph N. Mead:** Writing – review & editing, Supervision, Project administration, Methodology, Investigation, Funding acquisition. **Joseph R. Pawlik:** Writing – review & editing, Supervision, Project administration, Methodology, Investigation, Funding acquisition, Conceptualization.

Declaration of competing interest

The authors declare the following financial interests/personal relationships which may be considered as potential competing interests: Joseph Pawlik reports financial support was provided by National Science Foundation. If there are other authors, they declare that they have no known competing financial interests or personal relationships that could have appeared to influence the work reported in this paper.

Acknowledgement

Many thanks to Laura Gaitan Daza, Melissa Dionesotes, and Michael Wooster for assistance in the field, and the staff of Smithsonian Institution's Carrie Bow Cay Field Station in Belize for logistical support. We also thank the guest editor and two anonymous reviewers for their thorough evaluation and constructive feedback, which has improved the clarity and rigor of this manuscript. This research was funded in part by the National Science Foundation (OCE 2218863).

Appendix A. Supplementary data

Supplementary data to this article can be found online at https://doi.org/10.1016/j.orggeochem.2024.104922.

Data availability

Data will be made available on request.

References

Achlatis, M., Pernice, M., Green, K., de Goeij, J.M., Guagliardo, P., Kilburn, M.R., Hoegh-Guldberg, O., Dove, S., 2019. Single-cell visualization indicates direct role of sponge host in uptake of dissolved organic matter. Proceedings of the Royal Society B: Biological Sciences 286, 20192153. https://doi.org/10.1098/rspb.2019.2153.

Arif, J.M., Farooqui, A., Siddiqui, M.H., Al-Karrawi, M., Al-Hazmi, A., Al-Sagair, O.A., 2012. Novel bioactive peptides from cyanobacteria. In: ur-Rahman, A. (Ed.), Studies in Natural Products Chemistry. Elsevier, pp. 111–161.

Aronson, R.B., Precht, W.F., Toscano, M.A., Koltes, K.H., 2002. The 1998 bleaching event and its aftermath on a coral reef in Belize. Marine Biology 141, 435–447. https://doi.org/10.1007/s00227-002-0842-5.

Azam, F., Fenchel, T., Field, J., Gray, J., Meyer-Reil, L., Thingstad, F., 1983. The ecological role of water-column microbes in the sea. Marine Ecology Progress Series 10, 257–263. https://doi.org/10.3354/meps010257.

Bayona, L.M., Kim, M.-S., Swierts, T., Hwang, G.-S., de Voogd, N.J., Choi, Y.H., 2021. Metabolic variation in Caribbean giant barrel sponges: Influence of age and sea-depth. Marine Environmental Research 172. https://doi.org/10.1016/j.marenvres.2021.105503.

Brocke, H.J., Wenzhoefer, F., de Beer, D., Mueller, B., van Duyl, F.C., Nugues, M.N., 2015. High dissolved organic carbon release by benthic mats in a Caribbean reef ecosystem. Scientific Reports 5, 8852. https://doi.org/10.1038/srep08852.

Campana, S., Hudspith, M., Lankes, D., et al., 2021. Processing of naturally sourced macroalgal- and coral-dissolved organic matter (DOM) by high and low microbial abundance encrusting sponges. Frontiers in Marine Science 8. https://doi.org/10.3389/fmars.2021.640583.

Carlson, C.A., Hansell, D.A., 2015. Chapter 3 - DOM Sources, Sinks, Reactivity, and Budgets. In: Hansell, D.A., Carlson, C.A. (Eds.), Biogeochemistry of Marine Dissolved Organic Matter, Second Edition. Academic Press, pp. 65–126.

Chadwick, N.E., Morrow, K.M., 2011. Competition among sessile organisms on coral reefs. In: Dubinsky, Z., Stambler, N. (Eds.), Coral Reefs: an Ecosystem in Transition. Springer, Netherlands, pp. 347–371.

Chambers, M.C., Maclean, B., Burke, R., et al., 2012. A cross-platform toolkit for mass spectrometry and proteomics. Nature Biotechnology 30, 918–920. https://doi.org/10.1038/nbt.2377.

Chanas, B., Pawlik, J.R., 1997. Variability in the chemical defense of the Caribbean reef sponge *Xestospongia muta*. In: Lessios, H.A., Macintyre, I.G. (Eds.), Proceedings of the 8th International Coral Reef Symposium. Smithsonian Tropical Research Institute, Panama, pp. 1363–1368.

de Bakker, D.M., van Duyl, F.C., Bak, R.P.M., Nugues, M.N., Nieuwland, G., Meesters, E. H., 2017. 40 Years of benthic community change on the Caribbean reefs of Curaçao and Bonaire: The rise of slimy cyanobacterial mats. Coral Reefs 36, 355–367. https://doi.org/10.1007/s00338-016-1534-9.

de Goeij, J.M., Moodley, L., Houtekamer, M., Carballeira, N.M., van Duyl, F.C., 2008b. Tracing ^{13}C-enriched dissolved and particulate organic carbon in the bacteria-containing coral reef sponge *Halisarca caerulea*: Evidence for DOM-feeding. Limnology & Oceanograpy 53, 1376–1386. https://doi.org/10.4319/lo.2008.53.4.1376.

de Goeij, J., van den Berg, H., van Oostveen, M., Epping, E., van Duyl, F., 2008a. Major bulk dissolved organic carbon (DOC) removal by encrusting coral reef cavity sponges. Marine Ecology Progress Series 357, 139–151. https://doi.org/10.3354/meps07403.

de Goeij, J.M., van Oevelen, D., Vermeij, M.J.A., Osinga, R., Middelburg, J.J., de Goeij, A.F.P.M., Admiraal, W., 2013. Surviving in a marine desert: The sponge loop retains resources within coral reefs. Science 342, 108–110. https://doi.org/10.1126/science.1241981.

Deignan, L.K., Pawlik, J.R., López-Legentil, S., 2018. Evidence for shifting genetic structure among Caribbean giant barrel sponges in the Florida Keys. Marine Biology 165, 106. https://doi.org/10.1007/s00227-018-3355-6.

Dittmar, T., Koch, B., Hertkorn, N., Kattner, G., 2008. A simple and efficient method for the solid-phase extraction of dissolved organic matter (SPE-DOM) from seawater: SPE-DOM from seawater. Limnology & Oceanography Methods 6, 230–235. https://doi.org/10.4319/lom.2008.6.230.

Djoumbou Feunang, Y., Eisner, R., Knox, C., et al., 2016. ClassyFire: Automated chemical classification with a comprehensive, computable taxonomy. Journal of Cheminformatics 8, 61. https://doi.org/10.1186/s13321-016-0174-y.

Dührkop, K., Fleischauer, M., Ludwig, M., et al., 2019. SIRIUS 4: a rapid tool for turning tandem mass spectra into metabolite structure information. Nature Methods 16, 299–302. https://doi.org/10.1038/s41592-019-0344-8.

Dührkop, K., Nothias, L.-F., Fleischauer, M., et al., 2021. Systematic classification of unknown metabolites using high-resolution fragmentation mass spectra. Nature Biotechnology 39, 462–471. https://doi.org/10.1038/s41587-020-0740-8.

Evans, J.S., López-Legentil, S., Pawlik, J.R., Turnbull, I.G., Erwin, P.M., 2021. Molecular detection and microbiome differentiation of two cryptic lineages of giant barrel sponges from Conch Reef, Florida Keys. Coral Reefs 40, 853–865. https://doi.org/10.1007/s00338-021-02089-8.

Fiore, C.L., Jarett, J.K., Lesser, M.P., 2013. Symbiotic prokaryotic communities from different populations of the giant barrel sponge, *Xestospongia muta*. MicrobiologyOpen 2, 938–952. https://doi.org/10.1002/mbo3.135.

Fiore, C.L., Freeman, C.J., Kujawinski, E.B., 2017. Sponge exhalent seawater contains a unique chemical profile of dissolved organic matter. PeerJ 5, e2870.

Ford, A.K., Bejarano, S., Nugues, M.N., Visser, P.M., Albert, S., Ferse, S.C.A., 2018. Reefs under siege—the rise, putative drivers, and consequences of benthic cyanobacterial mats. Frontiers in Marine Science 5, 18. https://doi.org/10.3389/fmars.2018.00018.

Freeman, C.J., Easson, C.G., Fiore, C.L., Thacker, R.W., 2021. Sponge–microbe interactions on coral reefs: Multiple evolutionary solutions to a complex environment. Frontiers in Marine Science 8, 705053. https://doi.org/10.3389/fmars.2021.705053.

Gunasekera, S.P., Ritson-Williams, R., Paul, V.J., 2008. Carriebowmide, a New cyclodepsipeptide from the marine cyanobacterium *Lyngbya polychroa*. Journal of Natural Products 71, 2060–2063. https://doi.org/10.1021/np800453t.

Haas, A.F., Naumann, M.S., Struck, U., Mayr, C., el-Zibdah, M., Wild, C., 2010. Organic matter release by coral reef associated benthic algae in the Northern Red Sea. Journal of Experimental Marine Biology and Ecology 389, 53–60. https://doi.org/10.1016/j.jembe.2010.03.018.

Haas, A.F., Fairoz, M.F.M., Wegley Kelly, L., et al., 2016. Global microbialization of coral reefs. Nature Microbiology 1, 16042. https://doi.org/10.1038/nmicrobiol.2016.42.

Haug, K., Salek, R.M., Steinbeck, C., 2017. Global open data management in metabolomics. Current Opinion in Chemical Biology 36, 58–63. https://doi.org/10.1016/j.cbpa.2016.12.024.

Hentschel, U., Fieseler, L., Wehrl, M., Gernert, C., Steinert, M., Hacker, J., Horn, M., 2003. Microbial Diversity of Marine Sponges. In: Müller, W.E.G. (Ed.), Sponges (porifera). Springer, pp. 59–88.

Hoer, D.R., Gibson, P.J., Tommerdahl, J.P., Lindquist, N.L., Martens, C.S., 2018. Consumption of dissolved organic carbon by Caribbean reef sponges. Limnology and Oceanography 63, 337–351. https://doi.org/10.1002/lno.10634.

Hudspith, M., Rix, L., Achlatis, M., et al., 2021. Subcellular view of host–microbiome nutrient exchange in sponges: Insights into the ecological success of an early metazoan–microbe symbiosis. Microbiome 9, 44. https://doi.org/10.1186/s40168-020-00984-w.

Hughes, T.P., 1994. Catastrophes, phase shifts, and large-scale degradation of a Caribbean coral reef. Science 265, 1547–1551. https://doi.org/10.1126/science.265.5178.1547.

Jiao, N., Robinson, C., Azam, F., et al., 2014. Mechanisms of microbial carbon sequestration in the ocean—future research directions. Biogeosciences Discussions 11, 7931–7990. https://doi.org/10.5194/bgd-11-7931-2014.

Kido Soule, M.C., Longnecker, K., Johnson, W.M., Kujawinski, E.B., 2015. Environmental metabolomics: Analytical strategies. Marine Chemistry 177, 374–387. https://doi.org/10.1016/j.marchem.2015.06.029.

Kuhl, C., Tautenhahn, R., Böttcher, C., Larson, T.R., Neumann, S., 2012. CAMERA: an integrated strategy for compound spectra extraction and annotation of liquid chromatography/mass spectrometry data sets. Analytical Chemistry 84, 283–289. https://doi.org/10.1021/ac202450g.

Laus, G., 2001. Biological activities of natural halogen compounds. In: ur-Rahman, A. (Ed.), Studies in Natural Products Chemistry. Elsevier, pp. 757–809.
Letourneau, M.L., Hopkinson, B.M., Fitt, W.K., Medeiros, P.M., 2020. Molecular composition and biodegradation of loggerhead sponge *Spheciospongia vesparium* exhalent dissolved organic matter. Marine Environmental Research 162, 105130. https://doi.org/10.1016/j.marenvres.2020.105130.
Loh, T.-L., McMurray, S.E., Henkel, T.P., Vicente, J., Pawlik, J.R., 2015. Indirect effects of overfishing on Caribbean reefs: Sponges overgrow reef-building corals. PeerJ 3, e901.
Maliao, R.J., Turingan, R.G., Lin, J., 2008. Phase-shift in coral reef communities in the Florida Keys National Marine Sanctuary (FKNMS), USA. Marine Biology 154, 841–853. https://doi.org/10.1007/s00227-008-0977-0.
Marín, A., Ros, J., 2004. Chemical defenses in sacoglossan opisthobranchs: Taxonomic trends and evolutionary implications. Scientia Marina 68, 227–241. https://doi.org/10.3989/scimar.2004.68s1227.
Marquez, B.L., Watts, K.S., Yokochi, A., et al., 2002. Structure and absolute stereochemistry of hectochlorin, a potent stimulator of actin assembly. Journal of Natural Products 65, 866–871. https://doi.org/10.1021/np0106283.
McMurray, S.E., Finelli, C.M., Pawlik, J.R., 2015. Population dynamics of giant barrel sponges on Florida coral reefs. Journal of Experimental Marine Biology and Ecology 473, 73–80. https://doi.org/10.1016/j.jembe.2015.08.007.
McMurray, S.E., Johnson, Z.I., Hunt, D.E., Pawlik, J.R., Finelli, C.M., 2016. Selective feeding by the giant barrel sponge enhances foraging efficiency. Limnology and Oceanography 61, 1271–1286. https://doi.org/10.1002/lno.10287.
McMurray, S.E., Stubler, A.D., Erwin, P.M., Finelli, C.M., Pawlik, J.R., 2018. A test of the sponge-loop hypothesis for emergent Caribbean reef sponges. Marine Ecology Progress Series 588, 1–14. https://doi.org/10.3354/meps12466.
Mevers, E., Byrum, T., Gerwick, W.H., 2013. Parguerene and precarriebowmide, two classes of lipopeptides from the marine cyanobacterium *Moorea producens*. Journal of Natural Products 76, 1810–1814. https://doi.org/10.1021/np400347f.
Moitinho-Silva, L., Steinert, G., Nielsen, S., et al., 2017. Predicting the HMA-LMA Status in marine sponges by machine learning. Frontiers in Microbiology 8, 752. https://doi.org/10.3389/fmicb.2017.00752.
Moran, M.A., Kujawinski, E.B., Stubbins, A., et al., 2016. Deciphering ocean carbon in a changing world. Proceedings of the National Academy of Sciences 113, 3143–3151. https://doi.org/10.1073/pnas.1514645113.
Morinaka, B.I., Skepper, C.K., Molinski, T.F., 2007. Ene-yne Tetrahydrofurans from the Sponge *Xestospongia muta*. Exploiting a Weak CD Effect for Assignment of Configuration. Organic Letters 9, 1975–1978. https://doi.org/10.1021/ol0705696.
Nelson, C.E., Goldberg, S.J., Kelly, L.W., Haas, A.F., Smith, J.E., Rohwer, F., Carlson, C. A., 2013. Coral and macroalgal exudates vary in neutral sugar composition and differentially enrich reef bacterioplankton lineages. ISME Journal 7, 962–979. https://doi.org/10.1038/ismej.2012.161.
Noriega-Ortega, B.E., Wienhausen, G., Mentges, A., Dittmar, T., Simon, M., Niggemann, J., 2019. Does the chemodiversity of bacterial exometabolomes sustain the chemodiversity of marine dissolved organic matter? Frontiers in Microbiology 10. https://doi.org/10.3389/fmicb.2019.00215.
Olinger, L.K., Strangman, W.K., McMurray, S.E., Pawlik, J.R., 2021. Sponges with microbial symbionts transform dissolved organic matter and take up organohalides. Frontiers in Marine Science 8, 548. https://doi.org/10.3389/fmars.2021.665789.
Orjala, J., Gerwick, W.H., 1996. Barbamide, a chlorinated metabolite with molluscicidal activity from the Caribbean cyanobacterium *Lyngbya majuscula*. Journal of Natural Products 59, 427–430. https://doi.org/10.1021/np960085a.
Pawlik, J.R., Kernan, M.R., Molinski, T.F., Harper, M.K., Faulkner, D.J., 1988. Defensive chemicals of the Spanish dancer nudibranch *Hexabranchus sanguineus* and its egg ribbons: macrolides derived from a sponge diet. Journal of Experimental Marine Biology and Ecology 119, 99–109. https://doi.org/10.1016/0022-0981(88)90225-0.
Pawlik, J.R., Steindler, L., Henkel, T.P., Beer, S., Ilan, M., 2007. Chemical warfare on coral reefs: Sponge metabolites differentially affect coral symbiosis in situ. Limnology and Oceanography 52, 907–911. https://doi.org/10.4319/lo.2007.52.2.0907.
Pawlik, J.R., Burkepile, D.E., Thurber, R.V., 2016. A vicious circle? Altered carbon and nutrient cycling may explain the low resilience of Caribbean coral reefs. Bioscience 66, 470–476. https://doi.org/10.1093/biosci/biw047.
Pedler, B.E., Aluwihare, L.I., Azam, F., 2014. Single bacterial strain capable of significant contribution to carbon cycling in the surface ocean. Proceedings of the National Academy of Sciences 111, 7202–7207. https://doi.org/10.1073/pnas.1401887111.
Petras, D., Koester, I., Da Silva, R., et al., 2017. High-resolution liquid chromatography tandem mass spectrometry enables large-scale molecular characterization of dissolved organic matter. Frontiers in Marine Science 4, 405. https://doi.org/10.3389/fmars.2017.00405.
Pielou, E.C., 1966. The measurement of diversity in different types of biological collections. Journal of Theoretical Biology 13, 131–144. https://doi.org/10.1016/0022-5193(66)90013-0.
R Core Team, 2020. R: a language and environment for statistical computing.
Reiswig, H., 1974. Water transport, respiration and energetics of three tropical marine sponges. Journal of Experimental Marine Biology and Ecology 14, 231–249. https://doi.org/10.1016/0022-0981(74)90005-7.
Reiswig, H.M., 1981. Partial Carbon and Energy Budgets of the bacteriosponge *Verongia fistularis* (Porifera: Demospongiae) in Barbados. Marine Ecology 2, 273–293. https://doi.org/10.1111/j.1439-0485.1981.tb00271.x.
Rix, L., de Goeij, J.M., van Oevelen, D., Struck, U., Al-Horani, F.A., Wild, C., Naumann, M.S., 2017. Differential recycling of coral and algal dissolved organic matter via the sponge loop. Functional Ecology 31, 778–789. https://doi.org/10.1111/1365-2435.12758.
Rix, L., Ribes, M., Coma, R., et al., 2020. Heterotrophy in the earliest gut: a single-cell view of heterotrophic carbon and nitrogen assimilation in sponge-microbe symbioses. The ISME Journal 1–14. https://doi.org/10.1038/s41396-020-0706-3.
Robbins, S.J., Song, W., Engelberts, J.P., et al., 2021. A genomic view of the microbiome of coral reef demosponges. ISME Journal 15, 1641–1654. https://doi.org/10.1038/s41396-020-00876-9.
Rubin-Blum, M., Antony, C.P., Sayavedra, L., et al., 2019. Fueled by methane: deep-sea sponges from asphalt seeps gain their nutrition from methane-oxidizing symbionts. The ISME Journal 13, 1209–1225. https://doi.org/10.1038/s41396-019-0346-7.
Schellenberg, J., Reichert, J., Hardt, M., Schmidtberg, H., Kämpfer, P., Glaeser, S.P., Schubert, P., Wilke, T., 2019. The precursor hypothesis of sponge kleptocnidism: Development of nematocysts in Haliclona cnidata sp. nov. (Porifera, Demospongiae, Haplosclerida). Frontiers in Marine Science 5. https://doi.org/10.3389/fmars.2018.00509.
Schmitz, F.J., Gopichand, Y., 1978. (7E, 13ξ, 15Z)-14,16-dibromo-7,13,15-hexadecatrien-5-ynoic acid. A novel dibromo acetylenic acid from the marine sponge *Xestospongia muta*. Tetrahedron Letters 19, 3637–3640. https://doi.org/10.1016/S0040-4039(01)95017-8.
Schymanski, E.L., Jeon, J., Gulde, R., Fenner, K., Ruff, M., Singer, H.P., Hollender, J., 2014. Identifying small molecules via high resolution mass spectrometry: Communicating confidence. Environmental Science and Technology 48, 2097–2098. https://doi.org/10.1021/es5002105.
Shimura, H., Iguchi, K., Yamada, Y., Nakaike, S., Yamagishi, T., Matsumoto, K., Yokoo, C., 1994. Aragusterol C: A novel halogenated marine steroid from an Okinawan sponge, *Xestospongia* sp., possessing potent antitumor activity. Experientia 50, 134–136. https://doi.org/10.1007/BF01984951.
Simón-Manso, Y., Marupaka, R., Yan, X., Liang, Y., Telu, K.H., Mirokhin, Y., Stein, S.E., 2019. Mass spectrometry fingerprints of small-molecule metabolites in biofluids: building a spectral library of recurrent spectra for urine analysis. Analytical Chemistry 91, 12021–12029. https://doi.org/10.1021/acs.analchem.9b02977.
Smith, C.A., Want, E.J., O'Maille, G., Abagyan, R., Siuzdak, G., 2006. XCMS: processing mass spectrometry data for metabolite profiling using nonlinear peak alignment, matching, and identification. Analytical Chemistry 78, 779–787. https://doi.org/10.1021/ac051437y.
Sun, J., Xia, Y., 2023. Pretreating and normalizing metabolomics data for statistical analysis. Genes & Diseases 11, 100979. https://doi.org/10.1016/j.gendis.2023.04.018.
Suntornchashwej, S., Chaichit, N., Isobe, M., Suwanborirux, K., 2005. Hectochlorin and morpholine derivatives from the Thai sea hare, *Bursatella leachii*. Journal of Natural Products 68, 951–955. https://doi.org/10.1021/np0500124.
Swierts, T., Peijnenburg, K.T.C.A., de Leeuw, C.A., Breeuwer, J.A.J., Cleary, D.F.R., de Voogd, N.J., 2017. Globally intertwined evolutionary history of giant barrel sponges. Coral Reefs 36, 933–945. https://doi.org/10.1007/s00338-017-1585-6.
Taylor, M.W., Radax, R., Steger, D., Wagner, M., 2007. Sponge-associated microorganisms: evolution, ecology, and biotechnological potential. Microbiology and Molecular Biology Review 71, 295–347. https://doi.org/10.1128/MMBR.00040-06.
Thomas, T., Moitinho-Silva, L., Lurgi, M., et al., 2016. Diversity, structure and convergent evolution of the global sponge microbiome. Nature Communications 7. https://doi.org/10.1038/ncomms11870.
van Duyl, F.C., Moodley, L., Nieuwland, G., van Ijzerloo, L., van Soest, R.W.M., Houtekamer, M., Meesters, E.H., Middelburg, J.J., 2011. Coral cavity sponges depend on reef-derived food resources: Stable isotope and fatty acid constraints. Marine Biology 158, 1653–1666. https://doi.org/10.1007/s00227-011-1681-z.
van Duyl, F.C., Mueller, B., Meesters, E.H., 2018. Spatio–temporal variation in stable isotope signatures ($\delta^{13}C$ and $\delta^{15}N$) of sponges on the Saba Bank. PeerJ 6, e5460.
van Santen, J.A., Poynton, E.F., Iskakova, D., et al., 2022. The Natural Products Atlas 2.0: a database of microbially-derived natural products. Nucleic Acids Research 50, D1317–D1323. https://doi.org/10.1093/nar/gkab941.
Villamizar, E., Díaz, M.C., Rützler, K., Nóbrega, R.D., 2014. Biodiversity, ecological structure, and change in the sponge community of different geomorphological zones of the barrier fore reef at Carrie Bow Cay, Belize. Marine Ecology 35, 425–435. https://doi.org/10.1111/maec.12099.
Villegas-Plazas, M., Wos-Oxley, M.L., Sanchez, J.A., Pieper, D.H., Thomas, O.P., Junca, H., 2019. Variations in microbial diversity and metabolite profiles of the tropical marine sponge *Xestospongia muta* with season and depth. Microbial Ecology 78, 243–256. https://doi.org/10.1007/s00248-018-1285-y.
Wang, M., Carver, J.J., Phelan, V.V., et al., 2016. Sharing and community curation of mass spectrometry data with Global Natural Products Social Molecular Networking. Nature Biotechnology 34, 828–837. https://doi.org/10.1038/nbt.3597.
Weber, L., Armenteros, M., Kido Soule, M., Longnecker, K., Kujawinski, E.B., Apprill, A., 2020. Extracellular Reef Metabolites Across the Protected Jardines de la Reina, Cuba Reef System. Frontiers in Marine Science 7, 582161. https://doi.org/10.3389/fmars.2020.582161.
Wegley Kelly, L., Nelson, C.E., Petras, D., et al., 2022. Distinguishing the molecular diversity, nutrient content, and energetic potential of exometabolomes produced by macroalgae and reef-building corals. In: Proceedings of the National Academy of Sciences 119. https://doi.org/10.1073/pnas.2110283119.
Weisz, J.B., Hentschel, U., Lindquist, N., Martens, C.S., 2007. Linking abundance and diversity of sponge-associated microbial communities to metabolic differences in host sponges. Marine Biology 152, 475–483. https://doi.org/10.1007/s00227-007-0708-y.
Winters, A.E., White, A.M., Dewi, A.S., Mudianta, I.W., Wilson, N.G., Forster, L.C., Garson, M.J., Cheney, K.L., 2018. Distribution of defensive metabolites in nudibranch molluscs. Journal of Chemical Ecology 44, 384–396. https://doi.org/10.1007/s10886-018-0941-5.

Wooster, M.K., McMurray, S.E., Pawlik, J.R., Morán, X.A.G., Berumen, M.L., 2019. Feeding and respiration by giant barrel sponges across a gradient of food abundance in the Red Sea. Limnology and Oceanography 64, 1790–1801. https://doi.org/10.1002/lno.11151.

Yahel, G., Sharp, J.H., Marie, D., Häse, C., Genin, A., 2003. In situ feeding and element removal in the symbiont-bearing sponge *Theonella swinhoei*: Bulk DOC is the major source for carbon. Limnology and Oceanography 48, 141–149. https://doi.org/10.4319/lo.2003.48.1.0141.

Yooseph, S., Nealson, K.H., Rusch, D.B., et al., 2010. Genomic and functional adaptation in surface ocean planktonic prokaryotes. Nature 468, 60–66. https://doi.org/10.1038/nature09530.

Zhou, X., Lu, Y., Lin, X., Yang, B., Yang, X., Liu, Y., 2011. Brominated aliphatic hydrocarbons and sterols from the sponge *Xestospongia testudinaria* with their bioactivities. Chemistry and Physics of Lipids 164, 703–706. https://doi.org/10.1016/j.chemphyslip.2011.08.002.